Available online at www.sciencedirect.com
SCIENCE DIRECT®
Journal of Catalysis 226 (2004) 240–244
JOURNAL OF CATALYSIS
www.elsevier.com/locate/jcat

Research Note

Investigation of inverse shape selectivity in alkane adsorption on SAPO-5 zeolite using the tracer chromatography technique

J.F.M. Denayer *, A.R. Ocakoglu, J.A. Martens, G.V. Baron

Dienst Chemische Ingenieurstechniek, Vrije Universiteit Brussel, Pleinlaan 2, B-1050 Brussel, Belgium
Centrum voor Oppervlaktechemie en Katalyse, Katholieke Universiteit Leuven, Kasteelpark Arenberg 23, B-3001 Leuven, Belgium

Received 5 March 2004; revised 22 April 2004; accepted 14 May 2004

Abstract

Adsorption of linear and branched alkanes (C_4–C_8 range) on a microporous silicoaluminophosphate material (SAPO-5) was studied using the chromatographic technique at 353–573 K. Under these experimental conditions of low micropore occupancy specific branched molecules adsorb preferentially over the corresponding linear isomers. Such inverse shape selectivity was encountered with isobutane, isopentane, 3-methylpentane, 2,2-dimethylbutane, 2,3-dimethylbutane, and 2,2-dimethylhexane. Other skeletal isomers exhibit the conventional shape selectivity; i.e., their adsorption is less favorable compared to the linear alkane with the same carbon number. The occurrence of inverse shape selectivity versus conventional shape selectivity can be explained in terms of compensation between the adsorption enthalpy and entropy. The branched species that exhibit inverse shape selectivity have a higher adsorption enthalpy compared to the linear chains, counterbalancing the negative contribution of adsorption entropy to the adsorption equilibrium.

Keywords: Adsorption; Inverse shape selectivity; Adsorption enthalpy and entropy; Alkane

1. Introduction

Molecular shape selectivity refers to the ability of zeolite micropores to differentiate between guest molecules on the basis of their size and shape [1]. Molecular shape selectivity is essential to many industrial processes, in which zeolites are used to separate and/or selectively convert molecules into desired products [2,3]. According to the conventional shape selectivity concepts, adsorption of slender molecules is preferred over bulkier molecules, and diffusivity is determined by molecular diameters. For example, in MFI zeolite linear alkanes are preferentially adsorbed over branched isomers [4]. This less favorable adsorption for the branched isomer is generally attributed to steric hindrance effects, preventing branched alkanes to adopt an "ideal" adsorptive configuration.

In 1993, Santilli et al. reported that preferential adsorption of the bulkier molecule can occur in specific situations [5]. Those authors reported preferential adsorption of 2,2-dimethylbutane and 3-methylpentane from their mixture with *n*-hexane on the zeolites SAPO-5 and mordenite.

In order to explain this inverse adsorption behavior, Santilli et al. performed molecular simulations. Their results showed that the pore width of SAPO-5, viz. 0.72 nm, is such that it leads to better van der Waals (VDW) contact of the bulkier molecule with the pore walls. Thus inside SAPO-5 pores bulky branched alkanes are favored over their linear counterparts in terms of adsorption enthalpies. Despite its relevance for zeolite catalysis [6], the introduction of such a radical concept to the field of shape selectivity on zeolites did not receive much attention in the literature [7–10]. The computational approach of Santilli et al. was based on approximations of thermodynamic parameters and computational simplifications. Coulombic interactions were neglected, zeolite frameworks were represented by oxygen atoms, and low occupancy data were assumed to be valid at high pore filling. Most importantly, Santilli et al. neglected the entropic contribution to adsorption equilibrium and considered adsorption enthalpies only. In a recent study published in this journal, Schenk et al. modeled the adsorption of hexane isomers inside several zeolite structures, includ-

* Corresponding author. Fax: +32 2 629 32 48.
E-mail address: joeri.denayer@vub.ac.be (J.F.M. Denayer).

0021-9517/$ – see front matter
doi:10.1016/j.jcat.2004.05.018

ing AFI, the topological framework model of SAPO-5 [8]. Those authors used CBMC simulation techniques, which circumvented the majority of the drawbacks of the earlier calculations by Santilli et al. and accounted for entropic contributions.

At low loading, the adsorption enthalpy of 2,2-dimethylbutane was lower than that of *n*-hexane, whereas in the earlier simulations of Santilli et al. the opposite was concluded. The recent CBMC simulations [8] reveal a slight preference for 2,2-dimethylbutane adsorption over *n*-hexane because of a smaller entropy loss upon adsorption compared to the linear chain. At high loading of the zeolite with hydrocarbons, the selective uptake of 2,2-dimethylbutane becomes more pronounced because this molecule has a smaller effective length than *n*-hexane, and is packed more efficiently in the tubular pores of SAPO-5, leading to an additional entropic advantage. Thus, it was concluded that inverse shape selectivity inside SAPO-5 pores is related to entropic effects rather than to enthalpic effects. Furthermore, the prerequisite for a pronounced entropic effect to occur is that the zeolite pores be almost fully saturated. In the original work of Santilli et al. the pore filling was high and corresponded to 60% [5].

In the present work, we conducted a comprehensive adsorption study of a broad range of linear and branched alkanes (C_4–C_8 range) on SAPO-5 at very low coverage using the tracer chromatographic approach. The aim was to verify the occurrence of inverse shape selectivity on SAPO-5 at low coverage. Adsorption enthalpy and entropy were derived from the temperature dependence of the adsorption equilibria.

2. Materials, experimental procedure, and methodology

SAPO-5 (IUPAC structure type AFI) is a microporous silicoaluminophosphate material [11]. The pore network consists of one-dimensional, straight cylindrical channels of almost uniform cross section of ca. 0.72 nm. SAPO-5 was synthesized according to the method given in Ref. [12]. The molar gel composition was (diethanolamine): 0.3 SiO_2:Al_2O_3:P_2O_5:50 H_2O. The synthesis was performed at 200 °C for 192 h under agitation.

Low coverage adsorption properties of alkanes were determined using the gas chromatographic method. In this technique, pulses of the components of interest are injected in an inert gas flowing through the chromatographic column. The first moment of the response curve at the outlet of the column is directly related to the Henry adsorption constant. The details about the experimental procedure can be found elsewhere [4]. The temperature range for the experiments was 353–573 K.

The hydrocarbons were all of analytical grade (at least 99%) and used without further purification. Liquid pulses of 0.02 µl were injected, which is 2000–3000 times less than the total adsorption capacity of the SAPO-5 sample loaded in the chromatographic column. Although the local concentration in the retention front varies with time and position in the column, the fact that there was no effect of injection volume on the retention time guaranteed that the experiments were performed in the linear part of the isotherm, where mutual interactions between the adsorbed molecules are negligible.

The key quantity obtained from chromatographic measurements is a temperature-dependent quantity, the Henry adsorption constant (K'), which is proportional to the retention time of the examined molecule inside a zeolite filled column [4]. The adsorption enthalpy (ΔH) was derived from the temperature dependency of the K' values given by the van't Hoff equation. Henry adsorption constants were determined at 7–8 different temperatures. Linear regression of $\ln(K')$ versus $1/T$ yielded correlation factors larger than 0.9995, with standard errors on the adsorption enthalpy of less than 0.3 kJ/mol.

The Henry adsorption constant (K') is related to the Gibbs free energy of adsorption at low coverage (ΔG_0) via

$$\Delta G_0 = -RT \ln(K' \rho_c RT), \tag{1}$$

in which R is the universal gas constant, T (K) the absolute temperature, and ρ_c the framework density of the zeolite structure (kg/m^3) [8]. The framework density of SAPO-5 is calculated as 1.772 kg/m^3 assuming a perfect structure. The adsorption entropy (ΔS_0, J/(mol K)) was calculated using the experimentally determined adsorption enthalpies (ΔH_0) and the Gibbs free energy (ΔG_0):

$$\Delta G_0 = \Delta H_0 - T \Delta S_0. \tag{2}$$

The standard error on the calculated adsorption entropy was always smaller than 0.6 J/(mol K).

3. Results and discussion

Chromatographic experiments provide highly accurate and detailed information on the individual interactions between adsorbing species and the atoms that circumscribe the pore structure [13,14]. This technique is generally used to investigate adsorption at very low occupancies [15,16]. Whether our experiments were performed under low occupancies we concluded from preliminary tests with different amounts of injection. No dependence of the retention time on the amount of injection (from 0.005 to 0.02 µl) was observed for any of the adsorbates, which guaranteed that the experiments were performed at sufficiently low coverage to ensure operation in the Henry regime.

Fig. 1 depicts chromatograms of pentane and hexane isomers on the SAPO-5 column. These chromatograms display the separation ability of AFI-type pores at low coverage. In the investigated C_6 isomer mixture, 2,2-dimethylbutane is retained significantly longer than hexane, while 2-methylpentane elutes even earlier. The preferential adsorption of 2,2-dimethylbutane over hexane and 2-methylpentane is an example of inverse shape selectivity in the Henry regime.

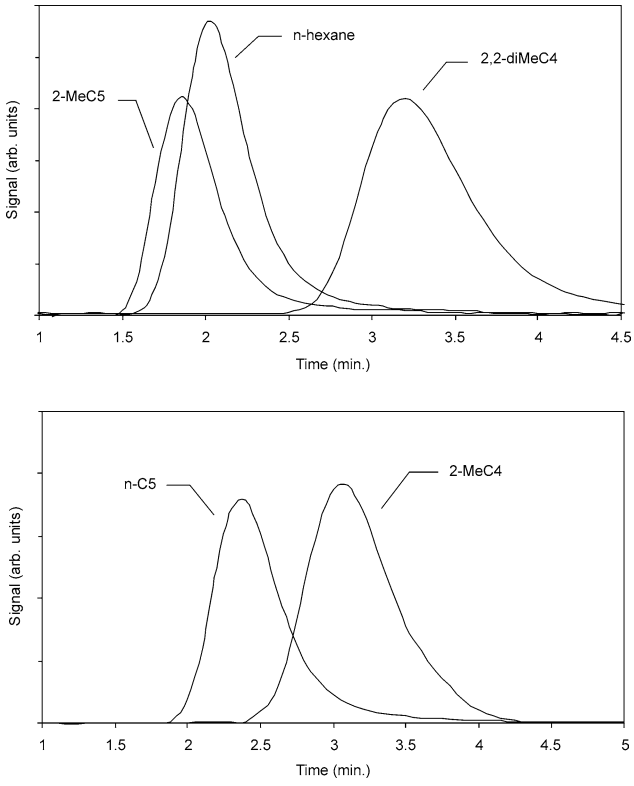

Fig. 1. Individual chromatograms of 2-methylpentane, *n*-hexane, and 2,2-dimethylbutane (top) and pentane and 2-methylbutane (bottom) on SAPO-5 at 150 °C.

Table 1
Henry constants, adsorption enthalpies, and entropies at zero coverage and separation factors of *n*- and iso-alkanes on SAPO-5

	K' (503 K) (mol/(kg Pa))	$-\Delta H_0$ (kJ/mol)	$-\Delta S_0$ (J/(mol K))	α
n-C_4	8.9×10^{-7}	37.9	117	
iso-C_4	9.2×10^{-7}	38.3	118	**1.03**
n-C_5	2.3×10^{-6}	45.3	124	
2-MeC_4	2.8×10^{-6}	46.8	125	**1.19**
n-C_6	6.8×10^{-6}	54.1	132	
2-MeC_5	6.1×10^{-6}	54.3	134	0.90
3-MeC_5	6.9×10^{-6}	55.0	134	**1.02**
2,2-diMeC_4	1.1×10^{-5}	56.8	134	**1.56**
2,3-diMeC_4	1.0×10^{-5}	56.6	134	**1.51**
n-C_7	2.2×10^{-5}	62.6	140	
2-MeC_6	2.0×10^{-5}	62.6	140	0.93
3-MeC_6	1.7×10^{-5}	62.8	142	0.78
2,3-diMeC_5	2.1×10^{-5}	64.3	143	0.97
2,4-diMeC_5	1.7×10^{-5}	63.8	144	0.81
n-C_8	7.4×10^{-5}	71.5	147	
2-MeC_7	6.8×10^{-5}	72.8	150	0.92
3-MeC_7	5.6×10^{-5}	72.3	151	0.76
4-MeC_7	3.5×10^{-5}	70.4	151	0.47
2,2-diMeC_6	7.5×10^{-5}	73.2	150	**1.01**
2,4-diMeC_6	5.2×10^{-5}	73.2	153	0.70
2,5-diMeC_6	7.0×10^{-5}	73.9	152	0.94
3,4-diMeC_6	4.7×10^{-5}	71.1	150	0.63
2,2,4-TriMeC_5	6.5×10^{-5}	73.1	151	0.88

Cases with inverse shape selectivity are indicated in bold.

The longer retention of hexane compared to 2-methylpentane is a common molecular shape-selective behavior (Fig. 1, top). Another example of inverse shape selectivity was encountered with pentane and 2-methylbutane. The branched molecule is longest retained in the SAPO-5 column (Fig. 1, bottom). We observed inverse shape selectivity for other isoalkane/*n*-alkane combinations as well. Table 1 summarizes the Henry constants and adsorption enthalpies and entropies, together with the separation factors (α) between linear and branched isomers. The separation factors (α) are obtained by dividing the Henry constant of the branched alkane by the Henry constant of the linear one. Inverse shape selectivity is detected by α values larger than unity. From the α values in Table 1 one can note that there is no straightforward relationship between occurrence of conventional versus inverse shape selectivity and carbon skeleton. For instance, inverse adsorption selectivity occurs with the singly branched isomers of butane and pentane. Among the six carbon alkanes, inverse shape selectivity occurs with 3-methylpentane, 2,2-dimethylbutane, and 2,3-dimethylbutane, but not with 2-methylpentane. None of the heptane isomers showed inverse shape selectivity. Out of eight studied branched octane isomers, only 2,2-dimethylhexane adsorbed preferentially over its linear counterpart, although the selectivity difference was subtle ($\alpha = 1.01$, Table 1).

Compensation charts in which adsorption entropy is plotted against adsorption enthalpy are a handy tool for analyzing the shape-selective phenomenon. For a homologous series of alkanes adsorbed on a given zeolite, the compensation chart is a straight line [16–18]. The physical meaning of this strict correlation between adsorption enthalpy and entropy is that the stronger a molecule interacts with the zeolite, the more freedom (entropy) it looses. At low occupancies, an alkane molecule that is trapped inside a micropore experiences VDW interactions with the pore walls. With alkanes, VDW interaction is the main contribution to the adsorption enthalpy. The VDW interaction depends on (1) the distance between the atoms of the molecule and the pore walls, and (2) the number and type of atoms in the molecule. The more the atoms of the molecule can be positioned at optimum distance from the pore walls, the higher the VDW interactions will be. Secondly, direct interactions between the acid site of the material and the alkanes via dipole-induced hydrogen bonding contribute to the total interaction [18]. The strength of this effect is nearly independent of the length of the alkane chain [18].

The freedom a molecule retains inside a zeolite micropore is governed by the ability to translate and rotate in the adsorbed state, which depends on the size and shape of the molecule and the pore topology. The individual contributions of enthalpy and entropy to the overall adsorption be-

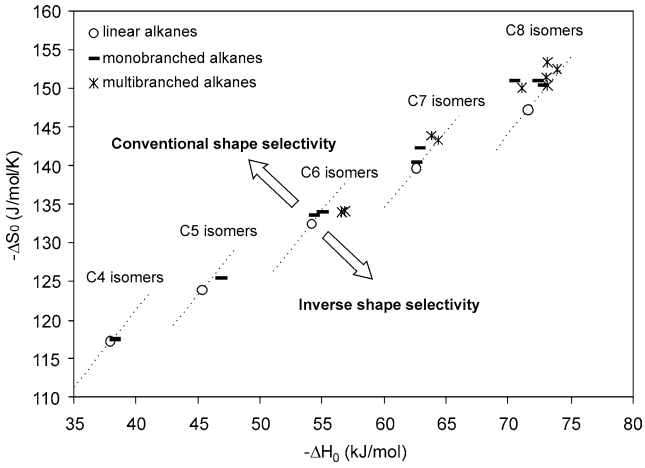

Fig. 2. Compensation chart of linear and branched alkanes on SAPO-5.

havior thus subtly depend on the steric fit between the guest molecule and the micropore.

Compensation charts for the molecules investigated are shown in Fig. 2. Nearly all branched isomers have higher adsorption enthalpies compared to the *n*-alkanes with the same carbon number, with a maximum difference of 2.7 kJ/mol (the values are listed in Table 1). These values reflect that branched alkane molecules exhibit a stronger interaction with the zeolite than linear alkanes. The critical diameter of a linear alkane chain is 4.3 Å, leaving a relatively wide free space between the molecule and the SAPO-5 pore walls, given the pore diameter of 7.2 Å. In previous investigations on zeolites having narrower pores [4,19–21], it was shown that much stronger VDW interactions can be obtained when the average distance between the alkane and the pore walls is narrowed down to ca. 0.5 Å. Side methyl groups on the alkane chain enable closer contact of hydrogen and carbon atoms with the pore walls, leading to stronger VDW interactions. For example, the critical diameter of 2,2-dimethylbutane is 6.3 Å, compared to 4.3 Å for a hexane. Alternatively, differences in polarizability of the C–H group between alkanes with secondary, tertiary, and quaternary carbon atoms could lead to differences in the direct dipole-induced hydrogen bonding between the acid sites of SAPO-5 and the alkane. However, experiments performed with $AlPO_4$-5 and its all-silica analogue SSZ-24 demonstrated that the adsorption enthalpy is similar on both materials for *n*- and iso-alkanes, indicating that the chemical composition and polarity have little influence on the interaction energy with this family of zeolites [22,23].

Although the energetic advantage holds for all branched isomers, not all of them exhibit inverse shape selectivity. Besides the advantageous enthalpic effect, branched molecules often have a more negative adsorption entropy compared to the *n*-alkanes (Table 1, Fig. 2). The presence of side groups on the chain reduces the freedom in the unidimensional SAPO-5 pores. Only those branched isomers having a more negative Gibbs free energy of adsorption than the *n*-alkanes, alkanes exhibit inverse shape selectivity. Hence, a criterion for $-\Delta S_0$ and $-\Delta H_0$ of the branched molecules which should be fulfilled to obtain inverse shape selectivity can be formulated using the compensation charts (Fig. 2). This criterion is based on the position of the experimental data point with respect to the line, crossing the data point of the linear alkane as shown in Fig. 2, dividing the $-\Delta S_0$ versus $-\Delta H_0$ field into two parts (see dotted lines in Fig. 2). Molecules on the line behave like the linear alkane and cannot be separated; i.e., there is no shape selectivity. Molecules having a combination of $-\Delta S_0$ and $-\Delta H_0$ values lying below this line have a lower Gibbs free energy of adsorption and a higher adsorption constant. This situation leads to inverse shape selectivity and is encountered with iso-butane, 2-methylbutane, 3-methylpentane, 2,2-dimethylbutane, and 2,3-dimethylbutane. For the other branched isomers, the gain in adsorption enthalpy compared to the linear chains is not

Table 2
Adsorption enthalpies and separation factors of *n*- and iso-alkanes on SAPO-5 from the literature

Reference	[5]	[5]	[10]	[9]	[8]	[8]	[This work]
Method	Pore probe	Molecular docking	CBMC, $AlPO_4$-5	Gravimetric	CBMC	CBMC	Chromatography
Fractional loading	0.6	0	0	~0.10	0	0.6	0
Temperature (°C)	130	150	30	30	130	130	230
ΔH *n*-C_6 − ΔH $2MeC_5$ (kJ/mol)	–	–	−53.4 − (−57.2) = **3.8**	−56.5 − (−62.2) = **5.7**	–		−54.1 − (−54.3) = **0.2**
ΔH *n*-C_6 − ΔH $3MeC_5$ (kJ/mol)	–	**1.71**	–	–	–	–	−54.1 − (−55.0) = **0.9**
ΔH *n*-C_6 − ΔH 2,2-diMeC_4 (kJ/mol)	–	**5.08**	–	−56.5 − (−67.8) = **11.3**	−54.0 − (−52.9) = **−1.1**		−54.1 − (−56.8) = **2.7**
ΔH *n*-C_6 − ΔH 2,3-diMeC_4 (kJ/mol)	–	–	–	−56.5 − (−66.5) = **10.0**	−54.0 − (−59.4) = **5.4**		−54.1 − (−56.6) = **2.5**
α $2MeC_5$/*n*-C_6[a]	–	–	2.79	1.28	–		0.90
α $3MeC_5$/*n*-C_6[a]	2.17	1.63	–	–	–	–	1.02
α 2,2-diMeC_4/*n*-C_6[a]	4.5	4.24	–	1.85 (40 °C)	1.31	4.07	1.56
α 2,3-diMeC_4/*n*-C_6[a]	~4	–		2.04	7.85		1.51

[a] The separation factor α is defined as (depending on the available data): the ratio of Henry adsorption constants or as the ratio of amounts adsorbed of the different molecules at a certain partial pressure.

large enough to compensate for the loss in entropy upon adsorption.

Table 2 summarizes adsorption properties of *n*-hexane, 2-methylpentane, 3-methylpentane, 2,2-dimethylbutane, and 2,3-dimethylbutane on SAPO-5, obtained with different experimental and simulation techniques. For 2-methylpentane, no experimental data at very low loading were found. At 10% zeolite loading, Newalkar et al. found that 2-methylpentane has a 5.7 kJ/mol stronger interaction than *n*-hexane, and is adsorbed selectively over the linear isomer, with a separation factor α of 2.79 [9]. Monte Carlo simulations by Fox et al. indicate that 2-methylpentane has a 3.8 kJ/mol higher interaction than *n*-hexane with $AlPO_4$-5, at zero loading [10]. The experiments of Santilli et al. with 3-methylpentane at about 60% zeolite loading indicate a separation factor of 2.17 [5]. Using the chromatographic technique, we found a very low selectivity for adsorbing 3-methylpentane over *n*-hexane at zero loading ($\alpha = 1.02$), and even no preference for adsorbing 2-methylpentane over *n*-hexane ($\alpha = 0.97$). Under these conditions, the interaction energy of 3-methylpentane is 0.9 kJ/mol higher than that of *n*-hexane.

Santilli et al. measured a pronounced preference for 2,2-dimethylbutane over *n*-hexane, with α equal to 4.2 at 60% zeolite loading. The simulations of Schenk et al. at this high loading lead to a quite similar α of 4.07, but predict a much lower α (1.31) at very low loading [8]. Newalkar et al. measured an α of 1.85 at 10% zeolite loading, while our chromatographic measurements at zero loading lead to $\alpha = 1.56$. Remarkable is that the experiments of Newalkar et al. and our experiments indicate that 2,2-dimethylbutane has a stronger interaction with the zeolite than *n*-hexane, while the simulations of Schenk et al. show the opposite (Table 2): a lower energetic interaction for the branched molecule at low loading, but also a lower loss of freedom compared to the linear chain. Despite this discrepancy between simulation and experiment, the selectivity at low loading obtained with both methods is comparable.

In this work, it is demonstrated that inverse shape selectivity occurs in SAPO-5 at very low micropore loading in the Henry regime. This inverse shape selectivity inside SAPO-5 micropores at low loading is a result of the more favorable energetic interaction of the branched alkanes with the pore walls. Inverse shape selectivity at low loading (α 2,2-diMeC_4/*n*-$C_6 = 1.6$) is clearly less pronounced than at high loading (α 2,2-diMeC_4/*n*-$C_6 = 4.5$). Entropic packing effects probably have to be invoked to explain the magnitude of the inverse shape selectivity at high loading, as indicated in the work of Schenk et al. [8].

Acknowledgments

J.F.M. Denayer is grateful to the F.W.O. Vlaanderen for a fellowship as postdoctoral researcher. This research was financially supported by F.W.O. Vlaanderen (G.0231.03N). The involved teams are participating in the IAP-PAI program for Supramolecular Chemistry and Catalysis, sponsored by the Belgian government. J.A. Martens acknowledges the Flemish Government for a concerted research action on the understanding of the elementary active site in catalysis.

References

[1] S.M. Csicsery, Pure Appl. Chem. 58 (1986) 841–856.
[2] N.Y. Chen, W.E. Garwood, F.G. Dwyer, Shape Selective Catalysis in Industrial Applications, Dekker, New York, 1989.
[3] T.F. Degnan Jr., J. Catal. 216 (2003) 32–46.
[4] J.F. Denayer, W. Souverijns, P.A. Jacobs, J.A. Martens, G.V. Baron, J. Phys. Chem. B 102 (1998) 4588–4597.
[5] D.S. Santilli, T.V. Harris, S.I. Zones, Micropor. Mater. 1 (1993) 329–341.
[6] J.A. Martens, P.A. Jacobs, in: H. van Bekkum, E.M. Flanigen, P.A. Jacobs, J.C. Jansen (Eds.), Studies in Surface Science and Catalysis, vol. 137, Elsevier Science, Amsterdam, 2001, Chap. 14.
[7] M. Schenk, S. Calero, T.L.M. Maesen, L.L. van Benthem, M.G. Verbeek, B. Smit, Angew. Chem. 114 (2002) 2610–2612.
[8] M. Schenk, S. Calero, T.L.M. Maesen, T.J.H. Vlugt, L.L. van Benthem, M.G. Verbeek, B. Schnell, B. Smit, J. Catal. 214 (2003) 88–99.
[9] B.L. Newalkar, R.V. Jasra, V. Kamth, S.G.T. Bhat, Adsorption 5 (1999) 345–357.
[10] J.P. Fox, V. Rooy, S.P. Bates, Micropor. Mesopor. Mater. 69 (2004) 9–18.
[11] W.M. Meier, D.H. Olson, Ch. Baerlocher, Atlas of Zeolite Structure Types, fourth ed., Elsevier Science, Amsterdam, 1996, pp. 26–27.
[12] B.M. Lok, C.A. Messina, R.L. Patton, R.T. Gajek, T.R. Cannan, E.M. Flanigen, U.S. patent 4,440,871 (1984) ex. 14.
[13] D. Atkinson, G. Curthoys, J. Chem. Educ. 55 (1978) 564–566.
[14] D.M. Ruthven, R. Kumar, Ind. Eng. Chem. Fundam. 19 (1980) 27–32.
[15] S.H. Hyun, R.P. Danner, AIChE J. 31 (1985) 1077–1085.
[16] A.R. Ocakoglu, J.F.M. Denayer, G.B. Marin, J.A. Martens, G.V. Baron, J. Phys. Chem. B 107 (2003) 398–406.
[17] F. Eder, J.A. Lercher, Zeolites 18 (1997) 75–81.
[18] F. Eder, M. Stockenhuber, J.A. Lercher, J. Phys. Chem. B 101 (1997) 5414–5419.
[19] F. Eder, J.A. Lercher, J. Phys. Chem. B 101 (1997) 1273–1278.
[20] J. Janchen, H. Stach, P.J. Grobet, J.A. Martens, P.A. Jacobs, Zeolites 12 (1992) 9–12.
[21] H. Stach, K. Fiedler, J. Janchen, Pure Appl. Chem. 65 (1993) 2193–2200.
[22] F. Eder, J.A. Lercher, J. Phys. Chem. B 100 (1996) 16460–16462.
[23] S.B. McCullen, P.T. Reischman, D.H. Olson, Zeolites 13 (8) (1993) 640–644.